A Neural Network Post-processing Approach to Improving NWP Solar Radiation Forecasts

Philippe Lauret, Hadja Maïmouna Diagne, Mathieu David

Available online at www.sciencedirect.com

ScienceDirect

Energy Procedia 57 (2014) 1044 – 1052

Energy Procedia

2013 ISES Solar World Congress

A Neural Network Post-processing Approach To Improving NWP Solar Radiation Forecasts

Philippe Lauret[a*], Maïmouna Diagne[a,b], Mathieu David[a]

[a]*PIMENT Laboratory, University of La Réunion, 15 Avenue Cassin, 97715 Saint-Denis, Réunion, France*
[b]*REUNIWATT company, Saint-Denis, 97400 Saint-Denis, Réunion, France*

Abstract

In this work, we investigate the use of artificial neural networks (ANNs) as a post-processing technique in order to improve mesoscale WRF solar radiation outputs.
More precisely, one day ahead (with a 1h temporal resolution) global horizontal irradiance (GHI) forecasts calculated by the WRF model are bias-corrected through the use of an ANN.
ANNs are data driven approaches capable of recognizing patterns in data. Training data obtained from a ground station are used to construct the ANN model in order to reduce the bias of the WRF forecasts. A bias error analysis allows the determination of the relevant ANN's inputs necessary to this bias correction. Among others, one can cite the solar zenith angle and the clear sky index.
This specific model output statistics (MOS) technique is applied in the frame of a solar PV forecasting project that takes place in La Reunion Island, a French oversea territory located in the Indian Ocean. This insular feature makes solar forecasting very challenging, hence the need for advanced solar forecasting methods

Keywords: Solar radiation forecasting; NWP model; MOS; Bias correction; Spatial averaging; Neural networks

1. Introduction

Solar radiation forecasting is of great importance for many applications such as, for instance, improved PV grid integration. More precisely, in order to increase the integration of renewables into electricity grids, accurate forecasts at various time steps (or forecast horizons) are needed. This statement is reinforced in the case of insular grids. Indeed, the intermittent character of the solar energy together with the fact that the island electricity grid is not connected may put in danger the stability of the grid and

* Corresponding author. Tel.: +262 262 93 81 27; fax: +262 262 93 86 65 .
E-mail address: philippe.lauret@univ-reunion.fr

doi:10.1016/j.egypro.2014.10.089

consequently the balance between supply and demand. In addition, solar forecasting may be very challenging in an insular context as islands (like Reunion Island for instance) may usually experience a high spatial and temporal variability of the solar resource.

Depending on the forecast horizon, different input data and forecasting models are appropriate. Time series models with on-site measured irradiance are adequate for the very short-term time scale ranging from 5 minutes up to 6 hours [1]. Forecasts based on cloud motion vectors from satellite images [2] show a good performance for a temporal range of 30 minutes to 6 hours. For forecast horizons from about 6 hours onwards, forecasts based on numerical weather prediction (NWP) models are generally more accurate [2]. Among the NWP models, a distinction is made between global models like GFS [3] or ECMWF [4] and regional or mesoscale models like WRF [5]. Global models usually have a coarse resolution and do not allow for a detailed mapping of small-scale features while mesoscale or regional models, which cover only a part of the planet, can be operated with a higher spatial resolution [2].

However, post-processing methods like model output statistics (MOS) or spatial averaging are frequently applied to refine the output of NWP models as detailed local weather features are generally not resolved by NWP predictions [2].

In this work, the weather research and forecasting (WRF) mesoscale model is used to forecast the day-ahead global horizontal irradiance (GHI). One year (2011) of forecasts is produced for the site of St Pierre (21°20'S ; 55°29'E) located in the southern part of Reunion Island. In order to improve the WRF solar radiation outputs, we investigate the use of artificial neural networks (ANNs) as a post processing technique. The first results show an improvement brought by this approach.

2. Context of the study

The station of St Pierre was selected to test the accuracy of the WRF forecasts. GHI is recorded every minute by a secondary standard pyranometer (CMP11 Kipp & Zonen). As solar forecasts were produced on an hourly basis, the one-minute ground data were averaged hourly as well.

Starting from initial conditions that are derived from worldwide observations given by the global forecasting model GFS, the WRF model generates forecasts over a final spatial resolution grid of 3km. Model runs are initiated each day at 1400 UTC and 30 hourly forecasts are made available. By discarding the first 6 hours, 24h ahead forecasts are extracted for grid points around the location of interest.

3. Post-processing of the irradiance forecasts

In order to obtain an optimized local prediction, post-processing techniques are used to refine the output of NWP models. Indeed, although spatial resolution has increased during the last years, the NWP models still do not resolve the local weather details [2]. Therefore, there is room for improvement as regards the original forecasts. Among the different post-processing approaches, one can cite Model Output Statistics (MOS) and spatial averaging.

3.1. Model Output Statistics

A post-processing technique like MOS can be used (among others) to reduce systematic forecast errors. The MOS technique consists in using ground irradiance measurements to correct localized errors from NWP models.

Consistent error patterns allow for MOS to be used to produce a bias reduction function for future forecasts [6]. For instance, as the original NWP forecasts showed a considerable overestimation of irradiance for intermediate sky conditions, Lorenz [7] modeled the bias correction function as a

polynomial function of the predicted clear sky index k_t^* and the solar zenith angle *SZA*. The corrected forecast is then obtained by subtracting the modeled bias from the original predicted values. This approach eliminated bias and reduced root mean square error (RMSE) of hourly forecasts by 5% for 24h forecasts.

3.2. Spatial averaging

As noted in [2], spatial averaging of irradiance forecasts can lead to improved forecast accuracy (and notably in terms of RMSE) by smoothing the variations in variable sky conditions (due to changing cloud cover). In this work, spatial averaging consists in predicting GHI for the station of St Pierre by taking the mean of the irradiance forecasts over 3 square grids centered on the station. Each square grid contains respectively 3-by-3, 5-by-5 and 7-by-7 irradiance forecasts. Each grid corresponds respectively to the following ground resolution: 9km, 15 km and 21 km. Following Pelland [8], the MOS correction method will be also applied to the spatially averaged WRF forecasts.

3.3. Neural network as a post-processing technique

Artificial Neural Networks (ANNs or simply NNs) are data driven approaches capable of performing a non-linear mapping between sets of input and output variables. The most popular form of neural network is the so-called multilayer perceptron (MLP) structure (see [9] for details). The MLP structure consists of an input layer, one or several hidden layers and an output layer. The input layer gathers the models inputs vector **x** while the output layer yields the models output vector *y*. Fig 1 represents a one hidden layer MLP.

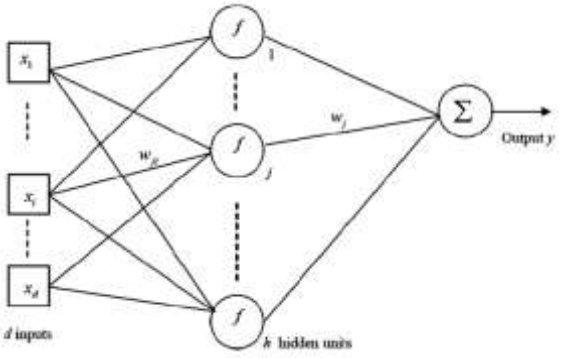

Fig. 1. Sketch of a MLP with d inputs and h hidden units, in our case, d=2 (clear sky index and cos(*SZA*). The output y is the modeled bias correction.

The hidden layer is characterized by several non-linear units (or neurons). The non-linear function (also called activation function) is usually the tangent hyperbolic function $f(x) = e^x - e^{-x} / e^x + e^{-x}$. Therefore, a neural network with *d* inputs, *h* hidden neurons and a single linear output unit defines a non-linear parameterized mapping from an input **x** to an output *y* given by the following relationship:

$$y = y(\mathbf{x};\mathbf{w}) = \sum_{j=0}^{h}\left[w_j f\left(\sum_{i=0}^{d} w_{ji} x_i \right) \right] \qquad (1)$$

The parameters of the NN model are given by the so-called weights and biases that connect the layers between them (notice that in Eq. 1, the biases are denoted by the subscripts $i = 0$ and $j = 0$ and are not represented in Fig 1). The NN parameters, denoted by the parameter vector **w**, govern the non-linear mapping. The NN parameters **w** are estimated during a phase called the training or learning phase. During this phase, the NN is trained using a dataset (called training set) of N input and output examples. The second phase, called the generalization phase, consists of evaluating the ability of the NN to generalize, that is to say, to give correct outputs when it is confronted with examples that were not seen during the training phase. Notice that these examples are part of a data set called test set.

As mentioned above, NNs has the appealing capability to recognize patterns in data. Indeed, NNs are able to approximate any continuous function at an arbitrary accuracy, provided the number of hidden neurons is sufficient. However, it is necessary to match the complexity of the NN to the problem being solved. The complexity determines the generalization capability (measured by the test error) of the model since a NN that is too complex will give poor predictions. In the NN community, this problem is called overfitting. Several techniques like pruning or Bayesian regularization [10] can be employed to control the NN complexity. In this work, we used the Bayesian Technique in order to control the NN complexity and therefore the generalization capability of the model [11].

In the realm of solar forecasting, NNs have been successfully applied to improve NWP output with respect to irradiance prediction. For instance, in [12], NNs have been used to reduce relative RMSE of daily average GHI by 15% when compared to original NWP forecasts.

In the present work, a NN is designed to derive the bias correction function. More precisely, the NN output (i.e. the modeled bias *BiasC*) is related to the predicted clear sky index k_t^* and the solar zenith angle *SZA*. The MOS-corrected WRF forecasts (WRF_c) are then obtained by subtracting the modeled bias from the original WRF forecasts (WRF_o):

$$WRF_c = WRF_o - BiasC \tag{2}$$

As mentioned above, the design of the NN requires a training dataset as well as a test set. Therefore, the original dataset has been divided in two distinctive parts. Finally, it is important to notice that this MOS correction is not applied for $SZA > 80°$.

4. Results

4.1. Bias error analysis of the original WRF forecasts

In order to derive a bias correction (i.e. correction of systematic deviations), a bias error analysis must be first conducted in order to reveal (or not) consistent error patterns. As mentioned by [2], the results of forecast evaluation will depend not only on the forecasting method but also on the climatic conditions at the selected site. Following Lorenz [7], a mean bias error (MBE) analysis in dependence of the clear sky index k_t^* (which is linked to the cloud situation) and the cosine of the solar zenith angle *SZA* (which is related to the daily course of the sun) has been made. This bias analysis is depicted in Fig 2.

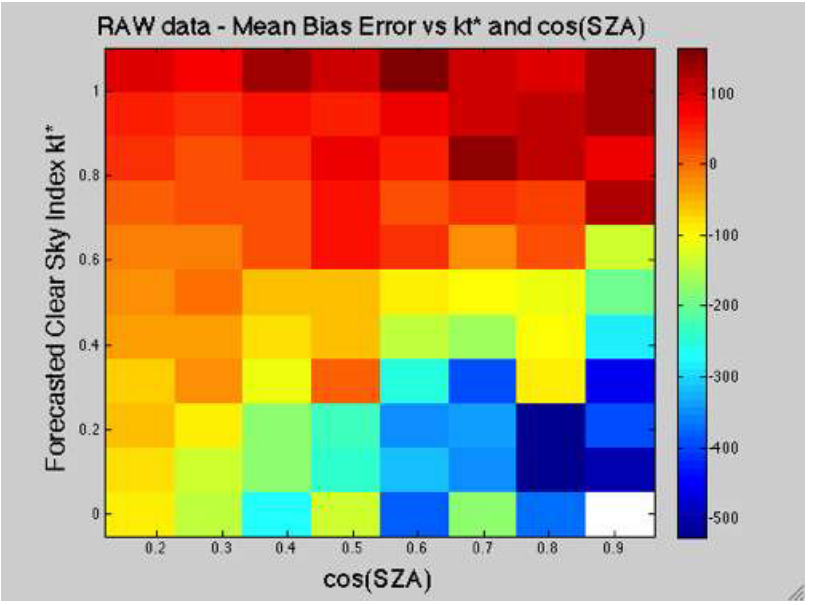

Fig. 2. MBE of original WRF forecasts as a function of *SZA* and forecasted clear sky index

Fig 2 shows that, for forecasted clear sky conditions ($k_t^* > 0.8$), WRF over-predicts ground measurement by up 160 W.m^{-2} and on average by 89 W.m^{-2}. For forecasted cloudy situations ($k_t^* < 0.8$), the WRF model under-predicts measured GHI by up -530 W.m^{-2} and on average by -140 W.m^{-2}. As expected, overall, the magnitude of the forecast errors increases with decreasing *SZA*.

Table 1 (line 1) gives the results of the original WRF forecasting model. The benchmarking of the different models is made according to the classical error metrics (see also appendix A) used by the solar forecasting community [13]. Notice that the night values are excluded in the computation of these error metrics. The relative values of the metrics are obtained by normalization to the mean ground measured irradiance of the considered period (mean value of GHI = 539.32 W.m^{-2}).

The results reported in Table 1 and the preceding bias analysis clearly demonstrate that WRF produces rather inaccurate forecasts. However, the bias analysis shows consistent MBE patterns and therefore motivates the design of a MOS correction function.

Table 1. Accuracy of the different forecasting methods

Method	RMSE (rRMSE)	MAE (rMAE)	MBE (rMBE)
Original WRF	189.81 (35.19%)	117.68 (21.82%)	51.44 (9.53%)
WRF+MOS-ANN	156.14 (28.95%)	115.51 (21.41%)	-1.39 (-0.25%)
WRF Avg. 3X3+MOS-ANN	156.37 (28.99%)	115.88 (21.48%)	-7.7 (-1.43%)
WRF Avg. 5X5+MOS-ANN	156.11 (28.94%)	116.52 (21.60%)	-9.31(-1.72%)
WRF Avg. 7X7+MOS-ANN	155.10 (28.76%)	115.74 (21.46%)	-9.74 (-1.8%)
Persistence	214.37 (39.74%)	142.97 (26.50%)	-0.29 (-0.05%)

4.2. MOS with a NN (one point forecast)

For this case study, the WRF forecast is extracted at the nearest point of the station of St Pierre. As mentioned above, an NN with 2 inputs (k_t^* and cos(*SZA*)) and one output (the modeled bias) was trained to establish the MOS correction function. An NN with 4 hidden units was designed and a Bayesian approach was applied to control the model complexity [11]. Corrections are made according to Equation (2) yielding a MOS-corrected WRF forecast.

Table 1 reports (for the entire dataset) the performance of the corrected model (denoted by WRF+MOS-ANN). Table 1 gives also the performances of a persistence model. Many versions for the persistence model are proposed in the literature [2]. In this work, for the persistence model, we chose to combine persistence of the clear sky index with the Bird clear sky model [14] (i.e. we combine measured clear sky index of the previous day with the clear sky model of the considered day).

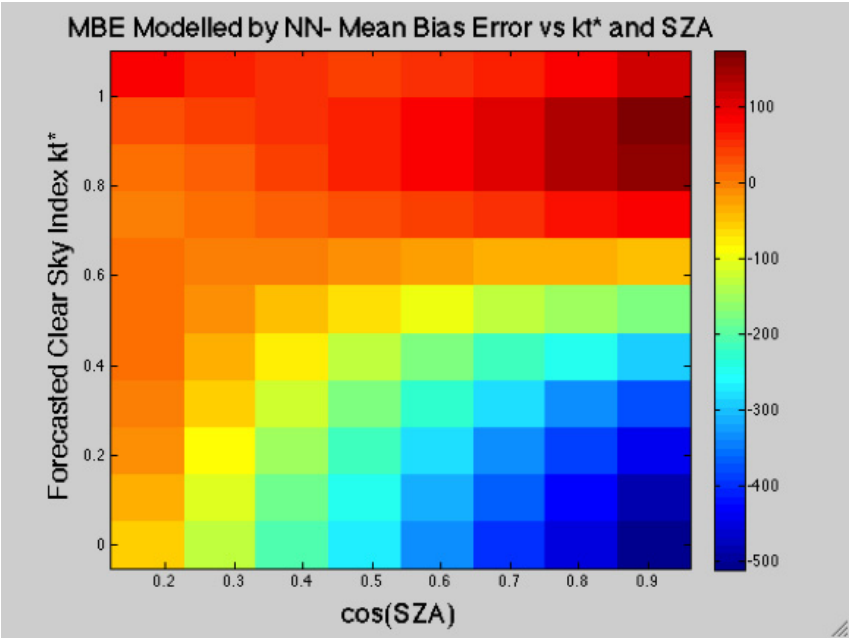

Fig. 3. MBE modeled by the ANN

Fig 3 plots the MOS correction modeled by the ANN. As seen, the ANN was quite able to capture the general trends of the data. Fig 4 displays the MBE of the MOS-corrected WRF. Fig 4 shows that for forecasted clear sky conditions ($k_t^* > 0.8$), the MOS-corrected WRF over-predicts ground measurement on average by 6 W.m^{-2}. For forecasted cloudy situations ($k_t^* < 0.8$), the MOS-corrected WRF model under-predicts measured GHI on average by -1 W.m^{-2}. On average, the bias of the MOS-corrected WRF is reduced to -76 W.m^{-2} to 0.7 W.m^{-2}.

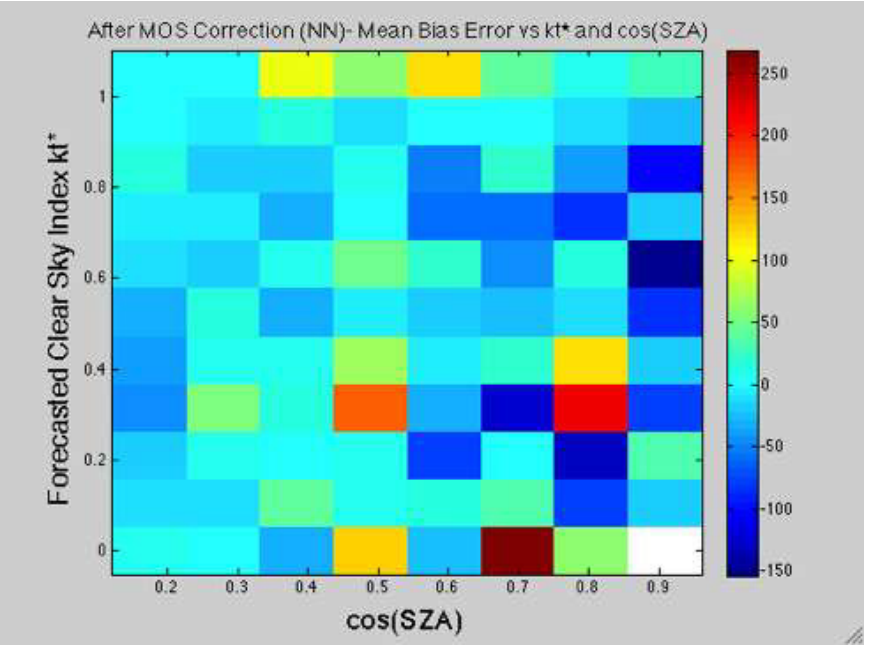

Fig. 4. MBE of the corrected forecast

Compared to the original WRF model, the corrected model WRF+MOS-ANN (as expected) shows a reduced bias. An improvement of the RMSE is also observed. One may suppose that the MOS correction method has also removed from the original forecasts some extreme outliers (or large error events). However, the MAE (which quantifies the tightness of the measure-model scatter plot near the 1-to-1 line) is slightly reduced.

4.3. MOS combined with spatial averaging

In this section, the spatially WRF averaged forecasts were used (instead of the one point forecast depicted in the previous section) as the starting point for the bias removal method. This spatial averaging technique consists in taking the mean of WRF forecasts over a square region centered on the location of the St Pierre station. Results are given for three averaged WRF forecast that corresponds respectively to the three square grids around St Pierre. The corresponding MOS-corrected WRF models are denoted by the acronyms WRF Avg. 3X3+MOS, WRF Avg. 5X5+MOS and WRF Avg. 7X7+MOS in Table 1. As reported in Table 1, this method led to similar results given by the bias removal with no spatial averaging.

5. Conclusion

In this study, a MOS correction technique based on ANNs is applied to correct original day-ahead WRF forecasts. By integrating local ground GHI measurements, the MOS method is used to remove the bias error from the mesoscale WRF model. A bias error analysis led to the design of an ANN-based correction function. Two approaches were investigated. The first one was based on only one point forecast while the second one was applied on spatially averaged WRF forecasts. The two methods led to similar results. While the MOS correction method led to a significant bias reduction, it appears that more

work must be done in order to improve the results. Several possibilities may be investigated. The first one may consist in using another global model like ECMWF to initialize the WRF model. The second may consist in carrying an in-depth study of the error analysis that could pinpoint in details the origin of the errors. This detailed error analysis may lead (in addition to the clear sky index and the *SZA*) to the definition of another relevant input variables for the ANN. In a perspective of regional forecasts, the third possibility would be to make use of satellite data (instead of a unique ground measurement) and averaged WRF forecasts to derive a so-called 'regional' MOS correction.

Acknowledgements

We acknowledge helpful discussions with Elke Lorenz (University of Oldenburg) and Richard Perez (ASRC- State University of New York).

References

[1] Reikard G. Predicting solar radiation at high resolutions: A comparison of time series forecasts. *Solar Energy* 2009; **83**:342-9.

[2] Lorenz E, Heinemann D. Prediction of solar irradiance and photovoltaic power. In: Sayigh A, editor. *Comprehensive Renewable Energy*, Oxford:Elsevier; 2012, p. 239-292

[3] GFS 2003. The GFS Atmospheric Model. http://www.emc.ncep.noaa.-gov/gmb/moorthi/gam.html

[4] ECMWF. http://www.ecmwf.int/research/.

[5] Skamarock W, Klemp J, Dudhia J, Gill D, Barker D, Wang W et al. A description of the advanced research WRF version 2. NCAR Technical Note NCAR/TN-468 +STR; 2007

[6] Mathiesen P, Kleissl J. Evaluation of numerical weather prediction for intra-day solar forecasting in the continental United States. *Solar Energy* 2011; **85**: 967–77.

[7] Lorenz E, Hurka J, Heinemann D, Beyer H. Irradiance forecasting for the power prediction of grid-connected photovoltaic systems. *IEEE Journal of Selected Topics in Applied Earth Observations and Remote Sensing* 2009; **2** :2–10.

[8] Pelland S, Gallanis G, Kallos G. Solar and photovoltaic forecasting through post-processing of the global environmental multiscale numerical weather prediction model. *Progress in Photovoltaics: Research and Applications* 2011; doi:10.1002/pip.1180.

[9] Bishop CM. Neural networks for pattern recognition. Oxford: Oxford University Press; 1995.

[10] MacKay DJC. A practical Bayesian framework for back-propagation networks. *Neural Computation* 1992; **4**:448–72.

[11] Lauret P, Fock E, Randrianarivony RN, Manicom-Ramsamy JF. Bayesian neural network approach to short time load forecasting. *Energy Conversion and Management* 2008; **49**:1156 -66

[12] Guarnieri R, Pereira EB, Chou SC. Solar radiation forecast using artificial neural networks in south brazil. Proceedings of ICSHMO, Foz do Iguaçu, Brazil, April 24-28, 2006, p. 1777-1785.

[13] Hoff TE, Perez R, Kleiss J, Renne D, Stein J. Reporting of irradiance modeling relative prediction errors. *Progress in Photovoltaics: Research and Applications* 2012; doi: 10.1002/pip.2225.

[14] Bird RE, Riordan C. Simple Solar Spectral Model for Direct and Diffuse Irradiance on Horizontal and Tilted Planes at the Earths Surface for Cloudless Atmospheres. *Journal of Climate and Applied Meteorology* 1986; **25:**87-97.

Appendix A. Definition of the error metrics and clear sky index

A.1. Definition of the error metrics

The following metrics RMSE (Root Mean Square Error), MAE (Mean Absolute Error) and MBE (Mean Bias Error) are used to benchmark the different solar forecasting models:

$$RMSE = \sqrt{\frac{1}{N}\sum_{i=1}^{N}\left(GHI_{forecast,i} - GHI_{measured,i}\right)^2}$$

$$MAE = \frac{1}{N}\sum_{i=1}^{N}\left|GHI_{forecast,i} - GHI_{measured,i}\right|$$

$$MBE = \frac{1}{N}\sum_{i=1}^{N}\left(GHI_{forecast,i} - GHI_{measured,i}\right)$$

where N is the number of points in the dataset for the considered period. Relative values of these metrics (*rRMSE*, *rMAE* and *rMBE)* are obtained by normalization to the mean ground measured irradiance of the considered period.

A.2. Definition of the clear sky index

$k_t^* = \frac{GHI}{GHI_{csk}}$ where GHI_{csk} is the output of a clear sky model (like the Bird clear sky model)